Structure and ultrastructure of neurospheres spontaneously generated in culture from sheep ovarian cortical cells.

Concepción Rojo Salvador
Universidad Complutense de Madrid Facultad de Veterinaria
Belén Sánchez-Maldonado
Universidad Complutense de Madrid Facultad de Veterinaria
María de Lourdes Galicia
Universidad Complutense de Madrid Facultad de Veterinaria
Alfredo González-Gil
Universidad Complutense de Madrid Facultad de Veterinaria
Rosa Ana Picazo González (rapicazo@ucm.es)
Universidad Complutense de Madrid Facultad de Veterinaria

Research article

Keywords: Spheroid, Neurosphere, Light cells, Dark cells, Ovarian cortical cells, Neural stem cells, Neural progenitors

Posted Date: December 6th, 2019

DOI: https://doi.org/10.21203/rs.2.18012/v1

Abstract

Background: Neurospheres derived from adult stem cells of non-neural tissues represent a promising source of neural stem cells (NSCs) and neural progenitor cells (NPCs) for autologous cell therapy in neurological diseases. Analyzing the fine structure of neurospheres can provide pivotal information regarding the phenotype of spheroid-integrating cells, being useful for cell characterization during differentiation, and oncogenic transformation. Neurospheres can be generated by culturing ovarian cortical cells under particular conditions. In order to assess the reliability of use of these spheroids in regenerative medicine, developmental biology, and to state whether they share morphological features with central nervous system (CNS) derived neurospheres, they were analyzed by light and transmission electron microscopy. Sheep ovarian cortical cells were cultured in serum-free medium for 21 days to generate neurospheres. On days 10, 15 and 21 of culture, expression of pluripotency (Nanog, Oct4, Sox2), and NSC/NPC (nestin, Pax6, P75NTR) transcripts by qRT-PCR, immunolocalization of NSC/NPC antigens (nestin, Pax6, P75NTR), structure, and ultrastructure, were analyzed in spheroids.

Results: Spheroids expressed transcripts and antigens of pluripotency, and NSC/NPC. Structural analyses revealed that cells were arranged in a peripheral sheet cover comprised by a few layers of spindle-shaped cells exhibiting frequent mitoses, and large round cells; and an inner core, with intermediate-sized cells showing frequent events of apoptosis and necrosis. Ultrastructural analyses showed that in the inner core, most cells were electron dense (dark), showing frequent apoptotic and degenerative events; the outer epithelium-like sheet, was formed by low electron dense cells (light flat cells; LFCs) showing signs of intense metabolic activity, abundant cytoplasmic organelles, phagosomes, lysosome-like structures, apical microvilli, and filament bundles of cytoskeleton elements, indicating that LFCs play a role in extracellular exchanges. Apical-basal polarization of LFCs evidenced by frequent intercellular contacts, like adherens junctions and cytoplasmic interdigitations, was lost in some cells whose contacts with neighboring cells were loose intedigitations and expanded cytoplasmic processes. This might anticipate disengaging/aggregating of light protruding cells (LPCs) from/to the neurosphere, as consistently observed in cultures by inverted microscopy.

Conclusions: Neurospheres spontaneously generated from ovarian cortical cells in culture, share most structural and ultrastructural characteristics of neurospheres derived from the CNS.

Background

Current progress in knowledge of stem cell physiology and stem cells-based therapies has improved the development of regenerative medicine. Even though rodent models have been widely used in stem cell studies, difficulties in the application of stem cell-based therapies in different species have led to investigate in domestic animals such as rabbits, pigs, sheep or non-humane primates [1]. For translational research purposes, stem cell-based therapy in large domestic animals requires detailed stem cell characterization and optimization of protocols for cell maintenance and differentiation [1]. For basic research purposes, using domestic species like sheep provides benefits related with the adequate size

and temperament of the animal. These characteristics facilitate surgical procedures that could eventually implement autologous cell therapy protocols in other physiologically similar species [2]. To assist this goal, alternative experimental models based on culture of stem cell spheroids provides a useful mean to characterize particular stem cells populations for their use as models for basic and translational research.

Recently, a culture system of neurospheres spontaneously generated from sheep ovarian cortical cells, has proven to be an eventually reliable experimental model for basic research in development, since it recapitulates some process occurring during neurogenesis, and neurosphere cells differentiate to give rise to neurons and glia [3]. The extra-neural origin of cells generating these neurospheres, emphasizes the interest of this alternative model for autologous stem cells therapy in regenerative medicine of the central nervous system. In addition, it provides a useful bioassay to investigate the pathogenesis of diverse prionic [4, 5], and non-prionic infectious diseases of the central nervous system in sheep and in several other species, as it has been done with the human Zika virus infection [6, 7], without the need to isolate cells from the neurogenic niches of the brain. This alternative model has a positive impact on the reduction of use of laboratory animals, since cells can be isolated from post-mortem ovaries, or after ovarian biopsies. This neurosphere-based model set up in sheep, would also be a reliable tool to test the effects of toxic substances or drugs on neurodevelopment of diverse domestic species and humans, as recommended by scientific and regulatory consensus [8].

Characterization of structure and ultrastructure of these spheroids is of great importance, since first, it would allow to assess whether these are similar to neurospheres derived from neurogenic niches of the central nervous system, and second, it would allow to establish standard criteria for comparison with those of pathological states.

Different studies have demonstrated that neurospheres and neurosphere-forming cells (NFCs) are morphologically heterogeneous when analyzing the cellular phenotypes with molecular markers and ultrastructure [9, 10]. This heterogeneity has been attributed to both the topographic distribution of cells within the spheroids and the presence of subpopulations of NFCs with distinct survival and proliferative behavior [9]. Lobo et al. [10] demonstrated the presence of two ultrastructurally and antigenically distinct populations of cells in neurospheres derived from rat fetal striatum: dark cells immunopositive for actin, weakly positive for vimentin and nestin-negative; and light cells immunopositive for actin, vimentin and nestin. Phagocytic and apoptotic events in sphere cells have also been described in these studies. The characteristics defining fetal and adult neural stem cells have been reviewed elsewhere [11]. Nestin is the main marker to identify neural precursors. However, it is not exclusive for neural stem cells (NSCs) even in neurospheres [11, 12], since cells considered as progenitors may be part of heterogeneous groups of proliferating cells. According to Bazán et al. [11] the ultrastructural features of NSCs are unknown because the only way to identify a single cell as a truly multipotent stem cell is to assay for self-renewal and multipotential capacities, but then the cells under study are lost since stem cells differentiate into their progeny. Subsequent studies have indicated that once the cell presents a series of prerequisites in terms of protein expression (i.e. responsiveness to growth factors and neurotransmitters or interaction

with the extracellular matrix through cell-cell interaction proteins) it has the biological tools necessary to proliferate, self-renew, and differentiate, regardless the identity of the expressed markers [13]. On the other hand, it has been considered critical to characterize in detail the morphology of expanded adult NSCs and neural progenitor cells (NPCs) [12] in order to assess the nature of the potentially transplanted cells to select the purest and healthiest populations, to expand them, and therefore to enhance the possibilities of success in cell replacement. Thus, it has been emphasized the importance of defining the morphological ultrastructure of neurospheres for the correct evaluation and optimization of cell culture conditions. Transmission electron microscopy (TEM) is considered as the most reliable method for assessing cell health in neurospheres [12] by identifying apoptosis and necrosis [10], or by showing slight ultrastructural changes at diverse organelles. However, the phenotype of the neurosphere cannot be described only by morphological criteria. TEM analysis has been very useful for characterization of NSCs in vivo, unlike for neurospheres generated in vitro. This is due to the undifferentiated state of cells exposed to the actions of growth factors added to culture medium, and to the clonal selection of particular cells towards a unique actively proliferating cell population occurring in culture. Thus, neurosphere cells do not represent adult NSCs [12]. Nevertheless, an interesting finding found by TEM in different neurosphere cell subpopulations has been the presence of cytoplasm filaments or annulate lamellae, closely placed around the nuclear membrane, and very often arranged in bundles. Also, a highly developed endoplasmic reticulum has been described [10, 12]. These features have been related to high proliferative activity of normal cells, (oocytes and embryonic cells) or tumor cells [14]. It has been proposed that cytoplasmic organelles could play a role as biosensors, by predicting graft survival and functionality after cell transplantation, or by detecting oncogenic transformation [12].

Vik-Mo et al. [15] carried out the first systematic study of sphere-organization in human neurospheres and tumorospheres. To elucidate the stem cell nature of spheroids they compared the ultrastructure of neurospheres and glioblastoma biopsies, and found clear similarities in the cellular phenotype and ultrastructure between normal and tumor derived neurospheres. They both contained a phenotypically heterogeneous cell population, that included the electronlucent and dense cells described in neurospheres from different species and sources [9, 10, 16, 17]. A difference was reported regarding the intermediate filament content in the cytoplasms of normal spheres that was more abundant than that in cells of tumorospheres. A model with differentiated cells residing in the periphery, and stem cells in the core, has been proposed for tumorospheres [15] in line with previous studies for normal neurospheres, having more mature cells at the periphery [9, 10, 18, 19]. It has been shown that maintenance of stem cell population is dependent on niches where anatomical organization coordinates stem cells function in space and time [20]. Such a niche has been described also in tumors, which may specify a self-renewing population of cells [21]. It has been proposed the possible generation of a niche within the spheres that allows the maintenance of stem cells in culture [15].

A recent contribution has shown that spheroids spontaneously generated in vitro from sheep ovarian cortical cells, exhibit molecular characteristics of neural stem/progenitor cells (NSCs/NPCs). These spheroids, when cultured under specific conditions, can self-renew and differentiate into neurons and glia, supporting their identity as neurospheres [3]. It would be of great interest to accomplish morphological

characterization of these neurospheres in order to elucidate whether they have similar features that are commonly found in normal or tumor neurospheres obtained from the central nervous system, likewise the presence of immature cells in the core and more mature cells at the periphery; the presence of subpopulations of electronlucent and electrondense cells; the presence of cytoplasmic intermediate filaments alone or in bundles; the frequent incidence of cell death phenomena (apoptosis and necrosis). The goal of this research was therefore, to identify the morphological hallmarks of neurospheres derived from sheep ovarian cortical cells, in order to determine whether they recapitulate similar structural and ultrastructural features of normal and tumor neurospheres from previous studies.

Results

Generation and development of spheroids in vitro

Cell aggregation was a consistent feature found from the first 24 h of culture, with generation of compact spheroids at approximately 7 days of culture (Fig.1A). These spheroids maintained similar diameters on days 10 (168.77 ± 13.05 μm), 15 (173.90 ± 14.69), and 21 (150.15 ± 11.81; Fig. 1L).

Observations under the inverted microscope allowed to evidence round cells with large nucleus to cytoplasm ratio that migrated towards, or arised from cell aggregates and spheroids (Fig. 1B,C). From day 10 onwards, a large number of cells exhibiting neural-like morphological characteristics were consistently placed around spheroids (Fig. 1D-K).

Alkaline phosphatase activity assay

Alkaline Phosphatase (AP) activity was consistently detected in all neurospheres generated in culture from day 5 onwards. At the end of culture period AP activity was predominantly localized on cells placed at the periphery of spheroids.

Gene expression analyses

Expression of pluripotent transcriptome represented by *Nanog*, *Oct4*, and *Sox2* (Fig. 2A) was evidenced in cell suspension before culture (day 0), and in all time-points of analysis during culture (days 10, 15, 21).

In cell suspension before culture, predominant expression was that of *Oct4*, with transcription levels higher than that of *brachyury*, *Nanog* and *Sox2* ($P < 0.01$), that were similarly expressed.

Expression of *Sox2* exhibited a robust increase ($P < 0.01$) over all other transcripts on day 10 in culture. *Sox2* expression remained higher ($P < 0.01$) than that of *brachyury* and *Nanog* on days 15 and 21 of culture, and similar to levels of transcription of *Oct4* in these two time-points.

In relation with transcripts characteristic of NSCs/NPCs (Fig. 2B), *nestin*, *Pax6* and *p75NTR* expression were detected and quantified in cell suspension before culture. Transcription of *nestin* and *p75NTR* was

significantly higher than expression of all other transcripts ($P < 0.01$) in cell suspension before culture, and at all time-points of analysis (days 10, 15 and 21 in culture).

Immunohistochemical localization of NSC/NPC antigens

Results of image analyses showing percentages of spheroid cells immunolocalizing the NSC/NPC antigens nestin, Pax6, and p75NTR, are summarized in Table 2.

Percentages of cells immunolocalizing nestin showed a time-dependent increase in culture that was significant on day 21 when compared with values quantified on day 10. Percentages of cells that immunolocalized Pax6 were similar on days 10, 15 and 21. Immunolocalization of p75NTR in spheroid cells, showed a time-dependent decrease in culture that was significant ($P < 0.01$) on day 21 when compared with percentages of localization of this antigen on days 10 and 15. Representative images are shown in Fig. 3.

Structural analysis of spheroids shows three morphologically different cell subpopulations

On day 10, most cell aggregates had a defined spherical shape (Fig. 4A) and only a few appeared as irregular cell clusters. Isolated cells that were partially attached to other cells at the spheroid periphery or located outside the sphere were consistently found. Spheroids showed a typical structure in which two areas could be distinguished: an outer sheet cover and an inner core area. The outer sheet cover was composed of spindle-shaped cells and large roud cells. Cells from the inner core area of each spheroid were separated by large intercellular spaces, with a moderate incidence of apoptosis and necrosis. Mitotic structures were mostly found in cells placed at the spheroid periphery. Cells were randomly distributed within the aggregates, with no particular organization. Although the cells exhibited variable morphology and size, three subpopulations of cells could be distinguished at all time-points: large round cells, intermediate-sized cells, and spindle-shaped cells.

Large round cells (Fig. 4A, arrow) were mainly located at the spheroid periphery or adjacent to but outside the spheroid and were either loosely or not attached to the aggregate. These cells had a large and eosinophilic cytoplasm, and a round excentric nucleus that had loosely extended chromatin and one or two large nucleoli. Spindle-shaped cells (Fig. 4A, star) were also present at the spheroid periphery and occasionally in the core of the sphere, and showed elongated nuclei. Intermediate-sized cells (Fig. 4A, arrowhead) were more frequently located in the core of the sphere. These cells had an irregular and slightly elongated nucleus with nuclear membrane invaginations, one or two nucleoli, and alternating areas of dispersed and condensed chromatin along the nuclear envelope. On day 15, the spheroids became large compact aggregates with a spherical shape (Fig. 4B) and more frequent signs of cell death manifested as apoptotic and necrotic cells mainly in the spheroid core. On day 21, the spheroids were smaller than those on day 15 and showed a round to oval morphology. Apoptotic phenomena and cellular debris were less evident than those on day 15.

Ultrastructural characterization of spheres

TEM analysis shows that spheres isolated from culture on days 15 and 21 have different sizes and a round to oval morphology with a semi-compacted cytoarchitecture. Spheres showed an apparent organization consisting of two well differentiated parts: a peripheral cover and an inner cell mass (Fig. 5A,B).

Cells lining the peripheral border were arranged in 2-3 layers resembling an epithelium. The superficial cells displayed two different patterns of cellular surface: a flat microvilli-bearing surface and a protruding-rounded microvilli-bearing surface (Fig. 5B,D). This different surface morphology (flat and protruding) was not associated with any apparent ultrastructural differences, although occasional protruding cells could be observed when exiting or aggregating with the sphere surface (Fig. 5C).

The inner mass in the spheres showed large intercellular spaces and irregularly shaped cells, although most of them were not randomly distributed but arranged around a central core (Fig. 5A,E). A few of these cells appeared dispersed, but many others were grouped showing a more compacted structure.

Although cells in the neurospheres exhibited morphological heterogeneity, two populations could be distinguished by TEM: dark and light cells.

Light cells showed low electron density and, although distributed throughout the sphere, they were more abundant in the periphery (Fig. 5D). Nuclei of these cells were large and round-shaped, frequently showing deep indentations of the nuclear envelope (Fig. 5F). The chromatin showed a dispersed pattern with few small aggregates of condensed chromatin masses along the nuclear envelope.

The cytoplasms of light cells were rich in free ribosomes and rough endoplasmic reticulum (RER), indicative of active intracellular synthesis (Fig. 5F,G). The RER appeared as well developed dilated cisternae, which were especially abundant next to the nucleus (Fig. 5G). Round or oval small mitochondria were also present, a few of them apparently showing degenerative signs such as swelling and loss of mitochondrial cristae (Fig. 5G). A constant characteristic finding in the cytoplasms of light cells was the presence of abundant intermediate filaments, either scattered or in bundles (Fig. 5G, 6A). Very common also was the finding of both lysosome and phagosomal vacuoles (Fig. 6B,C). The later contained some recognizable fragments of cytoplasmic organelles such as mitochondria (Fig. 6D,E). Both lysosome and phagosome-like structures were rare to find in the cytoplasms of the inner mass of cells.

Light cells in the peripheral lining of the neurosphere, either flat (LFCs) or protruding (LPCs), beared well-developed microvilli (Fig. 6F; see Fig. 5D, 7D). Underneath the microvilli, the apical cytoplasm of LFCs appeared more electrondense because of the presence of cytoskeleton elements (Fig. 6F).

Dark cells showed higher electron density than light cells and were more numerous in the core of the sphere (Fig. 7A,C,E). The ultrastructural characteristic of the nuclei of dark cells was the presence of nucleoli with a reticulated structural configuration (Fig. 7A,B,C; see Fig. 5E) which is indicative of active

protein synthesis. The cytoplasm of dark cells was exceptionally rich in large mitochondria, and RER cisternae. However, the abundance of cytoplasmic filaments found in light cells were not present in dark cells, and never arranged in bundles (Fig. 7B,C). Lysosome-like structures or phagosomes were also rarely found in dark cells.

Intercellular connections in the spheres varied according the location. In the core, cells with multiple processes scattered among the large intercellular spaces (see Fig. 5A), and cells forming more compact groups were in contact through close apposition of the cytoplasmic membranes (Fig. 7A,B,C; see Fig. 5E). At the spheroid periphery, the cells invariably established contact apically via adherens junctions (Fig. 7D; see Fig. 5F, 6C,F) and focal tight interdigitations (Fig. 7D; see Fig. 6F). More laterally, the cell surfaces had cytoplasmic processes loosely interdigitated with those from adjacent cells (Fig. 7D; see Fig. 5D, 6C).

Cell degeneration signs, abundant in the core of the sphere and compatible with early apoptosis, comprised increased cell density, chromatin condensation, membrane blebbing, higher incidence of cytoplasmic vacuoles and unrecognizable cell debris fragments (Fig. 7E-H; see Fig. 5E) as well as engulfment of cell debris by neighboring cells (Fig. 7F,H). Apoptotic bodies were not found. Degenerative and phagocytic phenomena were very common in neurospheres on day 21 of culture, not only in the sphere core but also on the periphery. Abundant vacuoles and intercellular spaces, either empty or occupied by lysosome-like vesicles and cytoplasmic content, were also identified (Fig. 7F,G,H).

Discussion

This work presents the structural and ultrastructural characterization of neurospheres derived from ovarian cortical cells in culture, under conditions previously established.

The identity of spheroid cells as NSCs/NPCs, was confirmed by their molecular signature, that comprised the expression of specific transcripts (nestin, Sox2, Pax6, p75NTR), and by the immunolocalization of the corresponding proteins (nestin, Pax6, p75NTR). A previous study has demonstrated that spheroids generated as described here are neurospheres, by the ability of their cells to self-renew and to differentiate into neurons and glial cells [3].

The pluripotent transcriptome, Sox2, Oct4 and Nanog, was consistently expressed by sphere cells at all time-points of analysis, which indicated their identity as stem cell spheroids. In addition, results showed a marked increase of Sox2 expression in spheroids sampled on day 10 in culture, in consistency with previous results [3]. Up regulation of Sox2 expression over that of Oct4 and Nanog, is characteristic of pluripotent stem cell specification to the neural lineage [22], whereby this increase of transcription would accompany this process. In fact, Sox2 is highly expressed in NSCs, and is down-regulated during their differentiation [23, 24], whereby Sox2 is normally considered as a NSC marker. At all time-points of analysis, during the whole culture period, nestin and p75NTR were the transcripts with highest expression. This is consistent with the identity of spheroid cells as NSCs/NPCs, since nestin, a protein that coassembles with vimentin to form class IV intermediate filaments [25] and participates in mechanisms of filaments disassembly during mitosis [26], is almost specifically expressed by NSCs, and used as

marker for neural precursor cells [27, 28]. As in previous studies [3], our results showed that 32–53% of spheroid cells showed positive nuclear immunolocalization of nestin. Nuclear localization of nestin, indicates a phosphorylated state of the protein that causes its depolymerization and transport into the nucleus [29]. Even though nestin is most commonly immunolocalized in cytoplasm, its nuclear localization occurs in highly proliferative cells such as in normal NSCs/NPCs during development [30], in NSCs/NPCs from postnatal CNS [31], and in cancer stem cells [32]. During neurogenesis, nestin expression is down-regulated, as development proceeds, being replaced by proteins characteristic of neurons and glia [33]. In the current study, a significant percentage of spheroid cells, predominantly placed in the outer sheet cover, show nestin immunolocalization at all time-points of analysis, indicating that NSCs, more immature multipotent cells, highly proliferative, and committed with the neural lineage, are present in these spheroids throughout the whole culture period.

p75NTR was expressed and localized during the entire culture period, as reported previously [3]. P75NTR is a common receptor for all neurotrophins, that partners with tyrosine kinase (TrK) receptors to regulate stem cell differentiation, apoptosis, migration and several other biological processes [34, 35]. p75NTR is particularly enriched in neural crest stem cells [36], and in neurosphere forming NPCs of diverse origin [37, 38, 39], whereby it is a bona-fide NSC/NPC marker.

Expression of Pax6, a specific transcript of neurogenesis [40, 41], increased on day 15 of culture over that of brachyury. Immunolocalization experiments evidenced that 84–94% of spheroid cells localized Pax6 protein, a NPC specific marker, that promotes NSCs/NPCs differentiation [42, 43], also in neurospheres [44].

Taken together, gene expression and immunolocalization analyses indicate that most spheroids cells co-localize at least two of the three NSC/NPC markers, in consistency with the previously established identity of these spheroids as neurospheres [3].

Defining the structural and ultrastructural features of in vitro-derived neurospheres of diverse origin is an essential analytical process for several reasons. First, because it can support the correct evaluation and optimization of cell culture conditions. Second, it can reveal the precise nature of the potentially transplantable cells [12], since from the analysis of cytoplasmic organelles by TEM, one can foretell graft survival and functionality after cell transplantation or detect oncogenic transformation. Finally, it can demonstrate the reliability of use of neurospheres derived from non-nervous system tissues in eventual cell therapy protocols, once established similar structural and ultrastructural indicators of these cells with respect to CNS derived neurospheres.

Results of structural and ultrastructural analyses, further support the demonstrated identity of these spheroids as neurospheres.

Results of histological analysis, and TEM on semi-thin sections of neurospheres derived from ovarian cortical tissue, revealed that cells were arranged in two well defined compartments: an outer sheet cover, and an inner core area.Three different cell populations were identified by light microscopy: large round

cells, intermediate-sized cells, and spindle-shaped cells. TEM analysis helped to elucidate the ultrastructural features of these cells that are consistent with morphological findings described earlier for neurospheres isolated from different tissues and species. Nevertheless, some differences can be appreciated.

The morphological heterogeneity of cells found in neurospheres of this study, has been widely described in neurospheres from central nervous system [9, 10, 11, 12]. Such cellular heterogeneity results, from the diverse topographic distribution of cells within the spheroid, and from the presence of cell subpopulations with distinct survival and proliferative behaviors [9].

Diverse phenotypes of neurosphere cells have been established by ultrastructural or/and antigenic characterization [9, 10, 11, 12, 16, 17]. Initially, two different cell phenotypes were identified in neurospheres: nestin-negative and nestin-positive cells [16]. Latter studies gave a more complete, but still imprecise, definition of NSCs.

The two main cell types identified by ultrastructural criteria in neurospheres of this study are light cells and dark cells. These cells have been previously described as dark cells, immunopositive for actin, weakly positive for vimentin and nestin-negative; light cells have been characterized as immunopositive for actin, vimentin, and nestin [10, 11]. An earlier study has shown that in these spheroids most nestin-positive cells are found at the spheroid periphery [3], where there was a major presence of “light cells”, with similar ultrastructural features, than those described by other authors [10, 11], along with abundance of adherens junctions. Results of TEM analyses carried out in the current research show similarities and some discrepancies with previous studies. Neurospheres from ovarian cortical tissue exhibited a core formed by irregularly shaped cells, immature cells, and dark cells, either healthy or degenerating. Most of the cells were arranged around a center, in which dark cells predominated and showed apposition of their cytoplasmic membranes with neighbouring cells, thus forming a compact mass of cells in the center. At the periphery, cells were arranged into epithelium-like layers mostly integrated by healthy mature light cells. These findings show coincidences with previous studies that identify a core of immature cells and an outer part of mature cells [9, 12]. We found a less marked random distribution of cells in the core of the sphere than that reported by other authors [10, 12]. Light cells in the outer part of the neurosphere exhibited two different morphologies: light non-protruding flat cells (LFCs), and light round protruding cells (LPCs). LPCs were shown by histological analyses, and TEM on semi-thin sections, to be leaving the spheroids or aggregating to them. LPCs corresponded to large round cells mentioned previously that were located at the periphery or even outside the spheroid, and were observed by inverted microscopy on days 10 and 15.

LFCs resembled an epithelium, which is supported by two findings: (a) the presence of intercellular junctions, (b) the presence of polarized light cells bearing abundant apical microvilli.

Our TEM results confirm that LFCs of the outer lining of neurospheres established adherens junctions. Adherens junctions have been the only type of cell junction reported in neurospheres, where it might play a role in cell aggregation, spheroid compaction and cell migration by formation of specific

cadherin/catenin/cytoskeleton complexes [10]. We found that adherens junctions were located between the apical and the basolateral membranes, serving as a boundary between apical and basal domains [45]. It is known that adherens junctions can be established as temporal cell attachments, to dynamically coordinate intercellular communication [46]. Both characteristics, temporality and high intercellular communication, are landmarks of sphere cells, which would explain the presence of adherens junctions.

In addition, we describe for the first time in neurospheres, the presence of two classes of intercellular contacts between neighbouring LFCs: what we refer to as apical tight interdigitations, and lateral loose interdigitations. Tight interdigitations found at the lateral membrane, were always placed at a very apical position, close to the adherens junction. Loose cellular interdigitations were consistently evidenced over the basal limit of the lateral membrane, beneath the adherens junctions. These types of cell contacts were only found between LFCs of the outer spheroid layer, where they might be participating in intercellular exchanges as can be deduced from the occurrence of multiple laterally expanded cytoplasmic processes, loosely interdigitated with those from adjacent cells through wide intercellular clefts. Such a finding has not been previously described in neurospheres. The only type of cell junction that has been reported is adherens junction, even though intercellular gaps void of cell expansions, and incomplete attachments have been also referred [10, 12]. The presence of the loose cellular interdigitations between LFCs, indicates that they maintain communication, while disengaging from the spheroid is occurring. Subsequently, cells protrude on the neurosphere surface (LPCs), and finally leave the sphere. During histological analyses, we have identified by light microscopy, LPCs on days 10 and 15, either loosely or not attached to the spheroids. In addition, time-course observations under the inverted microscope during spheroid culture, revealed the presence of a large number of round cells that arised from spheroids and migrated towards particular areas of the growth surface. Migrating round cells frequently showed filopodia and eventually, morphological features of neural cells. An alternative possibility is that, at least part of these round migrating cells, would be aggregating to a pre-existing spheroid. Our TEM results, add support to the first possibility, that will be addressed in future experiments. In any case, both migration followed by morphological differentiation, and migration followed by cell aggregation to generate a new spheroid most probably occur simultaneously, since prior studies have demonstrated that these spheroids self-renew, and their integrating cells are able to differentiate into neurons and glia [3]. Such cell disengaging at the lateral membranes seems to begin in the basal domain and to move towards the apical cell border, where adherens junctions and focal tight intedigitations are present, until the cell is finally released.

As we have already mentioned, LFCs placed at the outer spheroid layer exhibited signs of apical-basal polarity, such as the presence of apical microvilli and adherens junctions. Intercellular junctions play an essential role in maintaining apical-basal cell polarity since they serve as a physical limit between the apical/luminal and basolateral/luminal cell compartments [47]. Early cell-cell contacts during spheroid formation would induce the formation of intercellular junctions, which recruit and activate polarity proteins. In turn, polarity proteins regulate further maturation of adherens and tight junctions.

However, some observations might indicate that loss of polarization in LFCs could be underway on 15 days of culture. First, as we have already described the presence of loose interdigitations between neighbouring cells, seems to be reflecting cellular disengagement at this time (LPCs), which is a previous step for the cell to exit the sphere; loss of apical-basal polarity appears to be an essential requirement for cell disengaging, and is related with its proliferative activity and multipotency [48], being a characteristic feature of normal migrating cells, such as neural crest stem cells. Loss of apical-basal polarity is also characteristic of cells involved in tumor formation and metastasis [49, 50, 51, 52]. Second, we have shown that intermediate filaments were very abundant in light cells of neurospheres, particularly on day 15 of culture, when they were either strikingly spreaded out through the cytoplasm, in a non-polarized way, or arranged in bundles, as reported by Lobo et al. [10]. In other studies, intermediate filaments are mentioned as occasional findings [12]. In epithelial barriers, intermediate filaments provide mechanical strength and cellular shaping, and participate in maintenance and cross-talk with tight junction complexes [47, 53, 54, 55]. Intermediate filaments create polarized scaffolds to preserve epithelial asymmetry and cell shape [56]. As an example of such function, in ependymal cells, intermediate filaments together with apical F-actin bundles, maintain the structural integrity of the central canal [57]. In epithelial cells, intermediate filaments localize in apical regions, whereas in non-polarized multilayered epithelia their localization is ubiquitous. In fact, in non-polarized cells intermediate filaments are dynamic and mobile [56]. Even though the presence of filament bundles in the cytoplasm of light cells of neurospheres has been reported [10], their functional significance has not been yet explained. Our TEM results, along with observations under the inverted microscope, support the view that, since cell polarization in culture occurs slowly during several days, intermediate filaments might contribute to maintain structural integrity of spheroids for days.

Our results regarding arrangement of intermediate filaments in light cells of neurospheres, support the hypothesis that by day 15 of culture, loss of structural integrity and polarity of LFCs might be initiating, before LPCs leave the neurosphere. Therefore, we hypothesize that LFCs might become LPCs, and that progressive loss of apical-basal polarity would finally result in cell rounding prior to cell disengaging from the spheroid.

The abundance of intermediate filaments in light cells is supported by a previous study [3] in which most nestin (an intermediate filament protein) positive cells were more frequently found at the spheroid periphery, where light cells are more abundant.

Light cells placed at the outer sheet of the neurospheres (LFCs and LPCs), beared abundant microvilli at their apical membrane. The presence of apical microvilli is a characteristic feature of embryonic stem cells [58, 59, 60], epithelial cells of embryoid bodies [61], and neuroepithelial and neural progenitor cells during neurogenesis [62], but it has been reported to be a rare finding in neurospheres [12].

Apical microvilli found in light cells of the outer sheet cover from the current study, resembles those of ependymal cells. Microvilli of ependymocytes, considered as the source of multipotent adult NSCs [10, 63], provide the capability of adaptation of cells to different external conditions [57]. It is possible that

microvilli of outer sheet cover cells of the spheroid have a similar function, that is to become organized and positioned against external forces.

Cell rounding and the presence of microvilli, as shown in cells leaving the spheroids or aggregating to them, is a characteristic feature of progenitor cells that initiate migration with no adhesion to a growth surface [64]. Microvilli also function in absorption and secretion of molecules. The high metabolic activity of the light cells, evidenced by the abundance of cytoplasmic organelles, phagosomes and lysosome-like structures, correspond to the intense biochemical exchanges at the periphery of the sphere, as previously have been noted [9, 12], where the microvilli protrude.

Taken together, our results of TEM analysis of light cells of the outer sheet of the neurosphere, regarding polarity, intercellular junctions, and apical microvilli, seem to resemble that of epithelial cells of choroid plexus in the brain. These cells are the primary producers of the cerebrospinal fluid (CSF) and are responsible for establishing the blood–CSF barrier [65]. These cells display a characteristic polarity with microvilli, cilia and tight junctions at their apical side, and adherens junctions, gap junctions and desmosomes or basal infoldings at the basolateral side [66, 67, 68].

Within both dark and light cell populations, different phenotypes were identified: healthy dark cells, degenerating dark cells, flat light cells, protruding light migrating cells. Rather than subpopulations of cells [9], these cells might be transitional states from one or two original cell types that differentiated in culture within the spheroid.

Structural and ultrastructural results revealed that the outer layer comprises cells with signs of high metabolic activity, whereas the core of the neurosphere is the site of necrotic, apoptotic and phagocytic phenomena. These results are consistent with previous investigations showing high cell heterogeneity in the core, where apoptosis, necrosis and autophagy are frequent events, and the outer layer comprises healthier cells with intense protein synthesis and high mitosis rates [9, 12]. The compartimentalization of these phenomena may be related with the different capacity of the cells to reach culture medium nutrients and oxygen in the outer sheet or in the inner core of spheroids.

The increased incidence of degenerating cells, apoptotic phenomena, and phagocytic activity in the spheroid core, suggests that mechanisms for selection and elimination of overproduced cells are operating as autophagy-regulated phagocytosis [10] in this part of the spheroid. These mechanisms, known to function during development, contribute to eliminate apoptotic bodies during embryo differentiation [69].

Conclusions

From our results we can conclude that neurospheres spontaneously generated from ovarian cortical cells in culture, share most of structural and ultrastuctural characteristics of neurospheres derived from the CNS.

Methods

Cell culture

Ovaries were obtained from prepubertal ewe lambs (*Ovis aries*) aged 3 to 6 months that were sacrificed at a local abattoir close to the Complutense University, Veterinary Faculty in Madrid. Ovaries were dissected to obtain 1 mm-depth strips of cortex tissue that were dissociated as previously described [3]. Disaggregated tissue was filtered through 100 μm, 70 μm, and 40 μm cell-strainers (Beckton Dickinson, BD Falcon ref. 352360, ref. 352350, and ref. 352340, respectively) and cell viability of resulting suspension was assessed by Trypan blue staining (Sigma Aldrich, ref. T8154). Cells were cultured in fibronectin coated 24 microwell culture plates (Nunclon Delta, ref. 142475) at 500.000 alive cells per well, with 500 μl of culture medium M199 (Sigma Aldrich, ref. M7528) with 0.1% BSA (Sigma Aldrich, ref. A9418), L-glutamine (Sigma Aldrich, ref. G7513), insulin, transferrin, and selenium (ITS, Sigma Aldrich, ref. I3146), Synthecol (Sigma Aldrich, ref. S5442), and antibiotic-antimycotic (Gibco, Life Technologies, ref. 15240), during 21 days at 37 ˚C, 5% CO_2, and 99% humidity, as previously described [3].

Experimental designs

Time-course development of spheroids *in vitro* and morphometrical analysis were accomplished by twice-weekly image analysis of cultures. AP activity was analyzed once weekly from the 5th day of culture. For gene expression analyses, cell lysates were prepared on days 0, 10, 15, and 21 of culture. For histological and immunohistochemical analyses, spheroids were sampled and processed on days 10, 15, and 21. Spheroids were sampled and processed on days 15 and 21 of culture for TEM. Experiments were repeated three times, and results presented are mean values from these experiments.

Image analysis of spheroid development in vitro

Cultures were observed and photographed under an inverted microscope (Nikon Eclipse TiS), as previously described [3]. Time-course development of spheroids was depicted with twice-weekly measurements of diameters of at least 200 spheroids in each time-point.

Alkaline phosphatase activity assay

AP activity of spheroid cells was assessed once weekly after 5 days in culture with the aid of commercial reagents (Alkaline Phosphatase Detection Kit Millipore Cat. SCR004), as previously described [3].

Gene expression analyses

At each time-point, total RNA was extracted from lysates of cell spheroids, as previously described [3]. Lysates were stored frozen at -80ºC until RNA extraction, performed by passing lysates through

purification columns (Kit RNeasy mini kit, Quiagen, ref. 74104), followed by treatment with DNAse (Turbo DNA Free Kit, Ambion ref. AM1907). Transcripts corresponding to ovine *Oct4*, *Nanog*, *Sox2*, *nestin*, *Pax6*, *p75NTR*, *alpha-fetoprotein* (*AFP)*, *brachyury* and *18S ribosomal* RNA as endogenous control, were relatively quantified by qRT-PCR on days 0, 10, 15, and 21 in culture as previously described [3] in Servicio de Genómica y Proteómica Antonia Martín Gallardo (Parque Científico de Madrid, Campus de Cantoblanco). For amplification, primers were designed and synthesized, from available mRNA sequences at the National Center of Biotechnology Information, as shown in Table 1. For relative quantification of all transcripts at each time-point, levels of expression of *brachyury* were used as reference for normalization.

Light microscopy and Immunohistochemistry

Spheroids were processed for histology and immunohistochemistry following a procedure established in the laboratory (Patent P201300524/ PCT/ES2014/000089): culture medium was removed and cells were washed twice for 5 min with phosphate buffer solution (DPBS, Sigma Aldrich Química, ref. D8537) at 37 ˚C. Then, spheroids were fixed by addition of 4% paraformaldehyde in PBS (pH 7.4) for 15 min at 2-8 ˚C. The fixative was removed and cultures were washed twice for 5 min with ice-cold PBS, then sequentially dehydrated through an ascending series of ethanol (30%, 50% and 70%) (Merck Millipore, ref. 1009832500), 10 min each, at 2-8 ˚C. PBS washes, fixation, and dehydration were carried out on the culture plates under a stereo microscope (Nikon SMZ 800) with the aid of micropipettes (Steripette; Minitube International, ref. 19025/0050). Prior to paraffin embedding, spheroids were pre-aggregated in groups in 1% aqueous agar (Oxoid Ltd. Hampshire, England, ref. LP001) solution. The agar solution was then dispensed to form a continuous layer at the base of polypropylene molds (5 mm diameter x 3 mm depth). When the agar matrix solidified, spheroids were transferred from the culture wells to the mold a top the agar layer. Under a stereo microscope, excess ethanol was removed and spheroids were positioned at the center of the agar base using round-edge glass micropipettes before solubilized agar was added to overlay the grouped spheroids. Molds were incubated at 2-8 ˚C for 3-4 h until complete solidification of the agar. Agar blocks containing groups of spheroids were retrieved from the molds with 26-gauge syringe needles and placed into labeled histology cassettes for storage in 70% ethanol until paraffin embedding. Spheroid samples were sectioned into 4 µm slices and stained with hematoxylin and eosin. Immunohistochemical staining was based on the biotin peroxidase complex method, using a commercial kit (NovoLink Polymer Detection System, 250 tests, NRE7140-K, Leica Microsystems, United Kingdom) following the manufacturer's recommendations. Sections were pretreated with 10mM citrate buffer (pH 6.0) in a pressure cooker for antigen retrieval, cooled for 30 min at room temperature (RT) and washed twice in distilled water. Incubation with primary antibodies was carried out in a humidified chamber and the following antibodies and conditions were used: rabbit polyclonal anti-Pax6 antibody (ref. 030765, Sigma-Aldrich, Inc., Saint Louis, USA) diluted 1:400 and incubated overnight at 4 ˚C; rabbit polyclonal anti-nestin (ref. N5413 Sigma Aldrich, Inc., Saint Louis, USA) diluted 1:200 and incubated for 1 h at RT; mouse monoclonal anti-nerve growth factor receptor (p75NTR; ref.N3908, Sigma Aldrich, Inc., Saint Louis, USA) diluted 1:1,500 and incubated overnight at 4 ˚C. Immunolocalization was detected by exposure of tissue sections to 3-3'diaminobenzidine tetrachloride (DAB) for 5 min at RT. After washing for

10 min in distilled water, sections were counterstained with hematoxylin, dehydrated in alcohol, cleared and mounted. In negative control sections, protein block solution was used instead of primary antibodies in the corresponding incubation step. All primary antibodies were previously validated in our laboratory. At least 10 sections per timepoint were used for immunolocalization of each individual marker. Images of sections were obtained with an Olympus camera connected to an Olympus DP50 microscope and processed using Viewfinder Lite and Studio Lite software (Better Light Inc., San Carlos, CA). Positive and negative cells were counted in the images from each section obtained after immunohistochemistry, and the percentages of immunostained cells in each tissue section were calculated. Results are presented as mean percentage of immunostained cells at each timepoint with standard error of mean.

Transmission Electron Microscopy

Processing of spheres for TEM was carried out on days 15 and 21 of culture. Processing of samples collected on day 10 resulted in consistent tissue loss, and thus this time point was unsuitable for TEM analysis. Spheroids were fixed with 4% paraformaldehyde-0.5 glutaraldehyde in PBS for 2 h at RT. After rinsing with PBS, cells were post-fixed with 1% osmium tetroxide in PBS for 1 h, dehydrated by immersion in increasing concentrations of ethanol and acetone, and embedded in Epon 812 resin. A Leica-Reichert Ultracut E ultramicrotome was used to cut semithin (0.5 μm thick) and ultrathin (50-70 nm thick) sections that were then stained with methylene blue-azure and lead citrate-uranyl acetate, respectively. Sections were examined and photographed using a JeolJem 1010 transmission electron microscope at the Center of Transmission Electron Microscopy Luis Bru, Complutense University of Madrid.

Statistical analyses

The time-dependent variations of spheroid diameters in culture were analyzed by one-way analysis of variance (ANOVA), with $P < 0.01$ considered to be significant. Data for relative quantification of transcript expression levels using *brachyury* as reference gene at each time-point during culture were analyzed by one-way ANOVA, with $P < 0.01$ considered to be significant. The time-dependent variations in the percentages of immunolocalization of nestin, p75NTR, and Pax6 were determined by one-way ANOVA, with $P < 0.05$ considered to be significant. Bonferroni post-hoc test was performed after analysis of variance in all cases.

List Of Abbreviations

AFP: Alpha-fetoprotein; AP: Alkaline phosphatase; ANOVA: Analysis of variance: CSF: Cerebrospinal fluid; DAB: 3-3’diaminobenzidine tetrachloride; DPBS: Phosphate buffer solution; ITS: Insulin, transferrin, and selenium; LFCs: Light flat cells; LPCs: Light protuding cells; Nanog: Homeobox transcription factor; NFCs: Neurosphere-forming cells; NPCs: Neural progenitor cells; NSCs: Neural stem cells; Oct4: Octamer binding transcription factor 4; P75NTR: Neurotrophin receptor p75; Pax6: Paired box 6; RER: Rough endoplasmic reticulum; RT: Room temperature; Sox2: Sex determining region Y-box 2: TEM: Transmission electron microscopy; Trk receptor: Tyrosine kinase receptor.

Declarations

Ethics approval and consent to participate

Not applicable.

Consent for publication

Not applicable.

Availability of data and materials

The datasets used and/or analysed during the current study are available from the corresponding author on reasonable request.

Competing interests

The authors declare that no competing financial interest exist for the information contained in this manuscript.

Funding

This investigation was supported by the Ministerio de Economía y Competitividad, Gobierno de España, (Research Grant AGL/2008-03227), and by the Programa de Creación y Consolidación de Grupos de Investigación de la Universidad Complutense de Madrid (Research Group UCM-920380).

Authors' contributions

RP, CR and BS conceived and planned the experimentation. MG, AG,and RP, carried out the generation and development of spheroids *in vitro*, RNA extraction for qRT-PCR, and tissue processing for structural and immunohistochemical analyses; CR performed the ultrastructural characterization; BS and MG carried out the structural and immunohistochemical analyses. RP, CR, BS, and AG critically revised the manuscript. All authors participated in interpretation of results and helped to draft the manuscript.

Acknowledgments

We thank Pedro Aranda Espinosa and Agustín Fernández Larios for their technical support during sample processing for histology and immunohistochemistry, and TEM analyses, respectively; we are grateful to Silvia Vázquez Cuesta, Susana Ovalle, and Ricardo Ramos Ruiz for their expertise and technical support for qRT-PCR analyses, Ricardo García Mata for his work and collaboration on statistical analyses, and Javier Cebrián for his logistic support to achieve the goals of this research project.

References

1. Harding J, Roberts RM, Mirochnitchenko O. Large animal models for stem cell therapy. Stem Cell Res Ther. 2013; 4:23.
2. Scheerlinck JP, Snibson KJ, Bowles VM, Sutton P. Biomedical applications of sheep models: from asthma to vaccines. Trends Biotechnol. 2008;26:259-66.
3. Sánchez-Maldonado B, Galicia ML, Rojo C, González-Gil A, Flor-García M, Picazo RA. Spheroids spontaneously generated in vitro from sheep ovarian cortical cells contain integrating cells that exhibit hallmarks of neural stem/progenitor cells. Stem Cells Dev. 2018;27:1557-76.
4. Giri RK, Young R, Pitstick R, DeArmond SJ, Prusiner SB, Carlson GA. Prion infection of mouse neurospheres. Proc Natl Acad Sci U S A. 2006;103:3875-80.
5. Herva ME, Relaño-Ginés A, Villa A, Torres JM. Prion infection of differentiated neurospheres. J Neurosci Methods. 2010;188:270-5.
6. Garcez PP, Loiola EC, Madeiro da Costa R, Higa LM, Trindade P, Delvecchio R, Nascimento JM, Brindeiro R, Tanuri A, Rehen SK. Zika virus impairs growth in human neurospheres and brain organoids. 2016;352:816-8.
7. Rosa-Fernandes L, Cugola FR, Russo FB, Kawahara R, de Melo Freire CC, Leite PEC, Bassi Stern AC, Angeli CB, de Oliveira DBL, Melo SR, Zanotto PMA, Durigon EL, Larsen MR, Beltrão-Braga PCB, Palmisano G. Zika Virus Impairs Neurogenesis and Synaptogenesis Pathways in Human Neural Stem Cells and Neurons. Front Cell Neurosci. 2019;13:64.
8. Fritsche E, Grandjean P, Crofton KM, Aschner M, Goldberg A, Heinonen T, Hessel EVS, Hogberg HT, Bennekou SH, Lein PJ, Leist M, Mundy WR, Paparella M, Piersma AH, Sachana M, Schmuck G, Solecki R, Terron A, Monnet-Tschudi F, Wilks MF, Witters H, Zurich MG, Bal-Price A. Consensus statement on the need for innovation, transition and implementation of developmental neurotoxicity (DNT) testing for regulatory purposes. Toxicol Appl Pharmacol. 2018;354:3-6.
9. Bez A, Corsini E, Curti D, Biggiogera M, Colombo A, Nicosia RF, Pagano SF, Parati EA. Neurosphere and neurosphere-forming cells: morphological and ultrastructural characterization. Brain Res. 2003;993:18-29.
10. Lobo MV, Alonso FJ, Redondo C, López-Toledano MA, Caso E, Herranz AS, Paíno CL, Reimers D, Bazán E. Cellular characterization of epidermal growth factor-expanded free-floating neurospheres. J Histochem Cytochem. 2003;51:89-103.
11. Bazán E, Alonso FJ, Redondo C, López-Toledano MA, Alfaro JM, Reimers D, Herranz AS, Paíno CL, Serrano AB, Cobacho N, Caso E, Lobo MVT. In vitro and in vivo characterization of neural stem cells. Histol Histopathol. 2004;19:1261-75.
12. Gil-Perotín S, Durán-Moreno M, Cebrián-Silla A, Ramírez M, García-Belda P, García-Verdugo JM. Adult neural stem cells from the subventricular zone: a review of the neurosphere assay. Anat Rec (Hoboken). 2013;296:1435-52.
13. Maurer MH, Feldmann REJr, Bürgers HF, Kuschinsky W. Protein expression differs between neural progenitor cells from the adult rat brain subventricular zone and olfactory bulb. BMC Neurosci. 2008;9:7.

14. Morozova KN, Gubanova NV, Kiseleva EV. Structural organization and possible functional role of annulate lamellae containing cytoplasmic pores. Tsitologiia. 2005;47:667-78.
15. Vik-Mo EO, Sandberg C, Joel M, Stangeland B, Watanabe Y, Mackay-Sim A, Moe MC, Murrell W, Langmoen IA. A comparative study of the structural organization of spheres derived from the adult human subventricular zone and glioblastoma biopsies. Exp Cell Res. 2011;317:1049-59.
16. Kukekov VG, Laywell ED, Thomas LB, Steindler DA. **A nestin-negative precursor cell from the adult mouse brain gives rise to neurons and glia.** 1997;21:399-407.
17. Kukekov VG, Laywell ED, Suslov O, Davies K, Scheffler B, Thomas LB, O´Brien TF, Kusakabe M, Steindler DA. Multipotent stem/progenitor cells with similar properties arise from two neurogenic regions of adult human brain. Exp Neurol. 1999;156:333-44.
18. Suslov ON, Kukekov VG, Laywell ED, Scheffler B, Steindler DA. RT-PCR amplification of mRNA from single brain neurospheres. J Neurosci Methods. 2000;96:57-61.
19. Moe MC, Kolberg RS, Sandberg C, Vik-Mo E, Olstorn H, Yarghese M, Langmoen IA, Nicolaissen B. A comparison of epithelial and neural properties in progenitor cells derived from the adult human ciliary body and brain. Exp Eye Res. 2009;88;30-8.
20. Moore KA, Lemischka IR. Stem cells and their niches. Science. 2006;311:1880-5.
21. Sneddon JB, Werb Z. Location, location, location: the cancer stem cell niche. Cell Stem Cel 2007;1:607-11.
22. Wang Z, Oron E, Nelson B, Razis S, Ivanova N. Distinct lineage specification roles for NANOG, OCT4, and SOX2 in human embryonic stem cells. Cell Stem Cell. 2012;10:440-54.
23. Cavallaro M, Mariani J, Lancini C, Latorre E, Caccia R, Gullo F, Valotta M, DeBiasi S, Spinardi L, Ronchi A, Wanke E, Brunelli S, Favaro R, Ottolenghi S, Nicolis SK. Impaired generation of mature neurons by neural stem cells from hypomorphic Sox2 mutants. Development 2008;135:541-57.
24. Zhang S, Cui W. Sox2, a key factor in the regulation of pluripotency and neural differentiation. World J Stem Cells. 2014;6:305-11.
25. Eliasson C, Sahlgren C, Berthold CH, Stakeberg J, Celis JE, Betsholtz C, Eriksson JE, Pekny M. Intermediate filament protein partnership in astrocytes. J Biol Chem. 1999;274:3996-4006.
26. Chou YH, Khuon S, Herrmann H, Goldman RD. Nestin promotes the phosphorylation-dependent disassembly of vimentin intermediate filaments during mitosis. Mol Biol Cell. 2003;14:1468–78.
27. Lendahl U, Zimmerman LB, McKay RD. CNS stem cells express a new class of intermediate filament protein. 1990;60:585–95.
28. Dahlstrand J, Lardelli M, Lendahl U. Nestin mRNA expression correlates with the central nervous system progenitor cell state in many, but not all, regions of developing central nervous system. Brain Res Dev Brain Res. 1995;84:109-29.
29. Sahlgren CM, Mikhailov A, Hellman J, Chou YH, Lendahl U, Goldman RD, Eriksson JE. Mitotic reorganization of the intermediate filament protein nestin involves phosphorylation by cdc2 kinase. J Biol Chem. 2001;276:16456-63.

30. Merigo F, Mucignat-Caretta C, Zancanaro C. Timing of neuronal intermediate filament proteins expression in the mouse vomeronasal organ during pre- and postnatal development. An immunohistochemical study. Chem Senses. 2005;30:707-17.
31. Namiki J, Suzuki S, Masuda T, Ishihama Y, Okano Nestin protein is phosphorylated in adult neural stem/progenitor cells and not endothelial progenitor cells. Stem Cells Int. 2012;2012:430138.
32. Krupkova O, Loja TJr, Redova M, Neradil J, Zitterbart K, Sterba J., Veleska R. Analysis of nuclear nestin localization in cell lines derived from neurogenic tumors. Tumor Biol. 2011;32:631-9.
33. Zhang J, Jiao J. Molecular biomarkers for embryonic and adult neural stem cell and neurogenesis. Biomed Res Int 2015;2015:727542.
34. Meeker RB, Williams KS. The p75 neurotrophin receptor: at the crossroad of neural repair and death. Neural Regen Res. 2015;10:721-5.
35. Ioannou MS, Fahnestock M. ProNGF, but not NGF, switches from neurotrophic to apoptotic activity in response to reductions in TrkA receptor levels. Int J Mol Sci. 2017;18:E599.
36. Jiang X, Gwye Y, McKeow SJ, Bronner-Fraser M, Lutzko C, Lawlor ER. Isolation and characterization of neural crest stem cells derived from in vitro-differentiated human embryonic stem cells. Stem Cells Dev. 2009;18:1059-70.
37. Young KM, Merson TD, Sotthibundhu A, Coulson EJ, Bartlett PF. p75NTRneurotrophin receptor expression defines a population of BDNF-responsive neurogenic precursor cells. J Neurosci. 2007;27:5146-55.
38. Wilkinson DJ, Bethell GS, Shukla R, Kenny SE, Edgar DH. Isolation of enteric nervous system progenitor cells from the aganglionic gut of patients with Hirschsprung's disease. PLoS One. 2015;10:e0125724.
39. Mung KL, Tsui YP, Tai EW, Chan YS, Shum DK, Shea GK. Rapid and efficient generation of neural progenitors from adult bone marrow stromal cells by hypoxic preconditioning. Stem Cell ResTher. 2016;7:146.
40. Manuel MN, Mi D, Mason JO, Price DJ. Regulation of cerebral cortical neurogenesis by the Pax6 transcription factor. Front Cell Neurosci. 2015;9:70.
41. Thakurela S, Tiwari N, Schick S, Garding A, Ivanek R, Berninger B, Tiwari VK.

Mapping gene regulatory circuitry of Pax6 during neurogenesis. Cell Discov. 2016;2:15045.

42. Sakurai K, Osumi N. The neurogenesis-controlling factor, PAX6, inhibits proliferation and promotes maturation inmurine astrocytes. J Neurosci. 2008;28:4604–12.
43. Gómez-López S, Wiskow O, Favaro R, Nicolis SK, Price DJ, Pollard SM, Smith A. Sox2 and PAX6 maintain the proliferative and developmental potential of gliogenic neural stem cells in vitro. 2011;59:1588–99.
44. Hack MA, Sugimori M, Lundberg C, Nakafuku M, Götz M. Regionalization and fate specification in neurospheres: the role of Olig2 and Pax6. Mol Cell Neurosci. 2004;25:664-78.

45. Baum B, Georgiou M. Dynamics of adherens junctions in epithelial establishment, maintenance, and remodeling. J Cell Biol. 2011;192:907-17.
46. Ivanov AI, Naydenov NG. Dynamics and regulation of epithelial adherens junctions: recent discoveries and controversies. Int Rev Cell Mol Biol. 2013;303:27-99.
47. Worzfeld T, Schwaninger M. Apicobasal polarity of brain endothelial cells. J Cereb Blood Flow Metab. 2016;36:340-62.
48. Kerosuo L, Bronner-Fraser What is bad in cancer is good in the embryo: Importance of EMT in neural crest development. Semin Cell Dev Biol. 2012;23:320–32.
49. McCaffrey LM, Macara IG. Epithelial organization, cell polarity and tumorigenesis. Trends Cell Biol. 2011;21:727-35.
50. Linch M, Sanz-Garcia M, Rosse C, Riou P, Peel N, Madsen CD, Sahai E, Downward J, Khwaja A, Dillon C, Roffey J, Cameron AJ, Parker PJ. Regulation of polarized morphogenesis by protein kinase C iota in oncogenic epithelial spheroids. Carcinogenesis. 2014;35:396-406.
51. Yang CC, Graves HK, Moya IM, Tao C, Hamaratoglu F, Gladden AB, Halder G. Differential regulation of the Hippo pathway by adherens junctions and apical-basal cell polarity Proc Natl Acad Sci USA. 2015;112:1785-90.
52. Okuyama H, Kondo J, Sato Y, Endo H, Nakajima A, Piulats JM, Tomita Y, Fujiwara T, Itoh Y, Mizoguchi A, Ohue M, Inoue M. Dynamic change of polarity in primary cultured spheroids of human colorectal adenocarcinoma and its role in metastasis. Am J Pathol. 2016;186:899-911.
53. Romero-Ramos M, Vourc´h P, Young HE, Lucas PA, Wu Y, Chivatacarn O, Zaman R, Dunkelman N, El-Kalay A, Chesselet MF. Neuronal differentiation of stem cells isolated from adult muscle. J Neurosci Res. 2002;69:894-907.
54. Mii S, Uehara F, Yano S, Tran B, Miwa S, Hiroshima Y, Amoh Y, Katsuoka K, Hoffman RM. Nestin-expressing stem cells promote nerve growth in long-term 3-dimensional Gelfoam®-supported histoculture. PLoS One. 2013;8:e67153.
55. Jung J, Kim JW, Moon HJ, Hong JY, Hyun JK. Characterization of neurogenic potential of dental pulp stem cells cultured in xeno/serum-free condition: in vitro and in vivo assessment. Stem Cells Int. 2016;2016:6921097.
56. Oriolo AS, Wald FA, Ramsauer VP, Salas PJ. Intermediate filaments: a role in epithelial polarity. Exp Cell Res. 2007;313:2255-64.
57. Li YC, Bai WZ, Sakai K, Hashikawa Fluorescence and electron microscopic localization of F-actin in the ependymocytes. J Histochem Cytochem. 2009;57:741–51.
58. Sathananthan H, Pera M, Trounson A. The fine structure of human embryonic stem cells. Reprod Biomed Online. 2002;4:56–61.
59. Baharvand H, Matthaei KI. The ultrastructure of mouse embryonic stem cells. Reprod Biomed Online. 2003;7:330–5.

60. Yoo H, Kim E, Hwang SU, Yoon JD, Jeon Y, Park KM, Kim KJ, Jin M, Lee CK, Lee E, Kim H, Kim G, Hyun SH. Ultrastructural comparison of porcine putative embryonic stem cells derived by in vitro fertilization and somatic cell nuclear transfer. J Reprod Dev. 2016;62:177-85.
61. Alharbi S, Elsafadi M, Mobarak M, Alrwili A, Vishnubalaji R, Manikandan M, Al-Qudsi F, Karim S, Al-Nabaheen M, Aldahmash A, Mahmood A. Ultrastructural characteristics of three undifferentiated mouse embryonic stem cell lines and their differentiated three-dimensional derivatives: a comparative study. Cell Reprogram. 2014;16:151–65.
62. Marzesco AM, Janich P, Wilsch-Bräuninger M, Dubreuil V, Langenfeld K, Corbeil D, Huttner WB. Release of extracellular membrane particles carrying the stem cell marker prominin-1 (CD133) from neural progenitors and other epithelial cells. J Cell Sci. 2005;118:2849-58.
63. Gritti A, Vescovi AL, Galli R. Adult neural stem cells: plasticity and developmental potential. J Physiol Paris. 2002;96:81–90.
64. Ohnishi H, Sasaki H, Nakamura Y, Kato S, Ando K, Narimatsu H, Tachibana K. Regulation of cell shape and adhesion by CD34. Cell Adh Migr. 2013;7:426–33.
65. Kapur SK, Wang X, Shang H, Yun S, Li X, Feng G, Khurgel M, Katz AJ. Human adipose stem cells maintain proliferative, synthetic and multipotential properties when suspension cultured as self-assembling spheroids. Biofabrication. 2012;4:025004.
66. Cheng NC, Chen SY, Li JR, Young Short-term spheroid formation enhances the regenerative capacity of adipose-derived stem cells by promoting stemness, angiogenesis, and chemotaxis. Stem Cells Transl Med. 2013;2:584–94.
67. Oltolina F, Zamperone A, Colangelo D, Gregoletto L, Reano S, Pietronave S, Merlin S, Talmon M, Novelli E, Diena M, Nicoletti C, Musarò A, Filigheddu N, Follenzi A, Prat M. Human cardiac progenitor spheroids exhibit enhanced engraftment potential. PLoS One. 2015;10:e0137999 (**This article has been corrected in PloS One.2015;10:e0141632).**
68. Campos Y, Qiu X, Gomero E, Wakefield R, Horner L, Brutkowski W, Han YG, Solecki D, Frase S, Bongiovanni A, d'Azzo A. Alix-mediated assembly of the actomyosin-tight junction polarity complex preserves epithelial polarity and epithelial barrier. Nat Commun. 2016;7:11876. .
69. Qu X, Zou Z, Sun Q, Luby-Phelps K, Cheng P, Hogan RN, Gilpin C, Levine B. Autophagy gene-dependent clearance of apoptotic cells during embryonic development. Cell. 2007;128:931–46.

Tables

Table 1 Primers used for qRT-PCR of transcripts expressed by neurospheres derived from sheep (*Ovis aries*) ovarian cortical cells. *AFP,* alpha fetoprotein.

Transcript	Accession number	Primers
Oct4	JN625522	F: CAAATCAGCCACATCGCC R: AGAACCACACTCGGACCA
Nanog	FJ970651.1 Exon 2-3	F: GCACAGAGAAGGAAGAGAAGG R: GCTGGAGACTGAGGTATTTCTG
Sox2	X96997.1	F: GGAGGACAGCAAGAAACAG R: GCGTGAGTGTAGATGGGA
Nestin	XM_004002626.1	F: CTCCAGAACTACTAAAGCCTACAG R: CCAGCGACTCTTGACTTTCC
p75NTR	XM_004013355.1	F: CTCATCCCTGTCTATTGCTCCA R: TTCCACCTCTTGAAGGCGA
Pax6	XM_004016373.1	F: AACATCCTTTACCCAAGAGCA R: TTTCTCGGGCAAACACATCTG
AFP	XM_004009903.1	F: ATGAATACTCAAGAAGACACCCAG R: CGAACCACTCTTTGAAATATCCC
Brachyury	XM_004011450.1	F: AACGCCATGTACTCCTTCCT R: CCCGTTCACGTACTTCCAG

Table 2 Percentages of spheroid cells showing immunolocalisation of NSC/NPC antigens nestin, Pax6, and p75NTR throughout time in culture in spontaneously generated spheroids derived from ovarian cortical cells *in vitro*. Data are mean values accompanied by standard error of mean. Different letters, and different number of asterisks indicate significant differences among mean values at $P < 0.05$, and $P < 0.01$, respectively. NSC, neural stem cells; NPC, neural progenitor cells.

DAYS IN CULTURE	NESTIN (%)	PAX6 (%)	P75NTR (%)
10	31.81 ± 3.04[a]	88.24 ± 2.64	81.85 ± 2.63*
15	49.53 ± 7.16	94.18 ± 0.81	78.48 ± 5.92*
21	53.07 ± 6.32[b]	84.43 ± 8.45	37.13 ± 5.01**

Figures

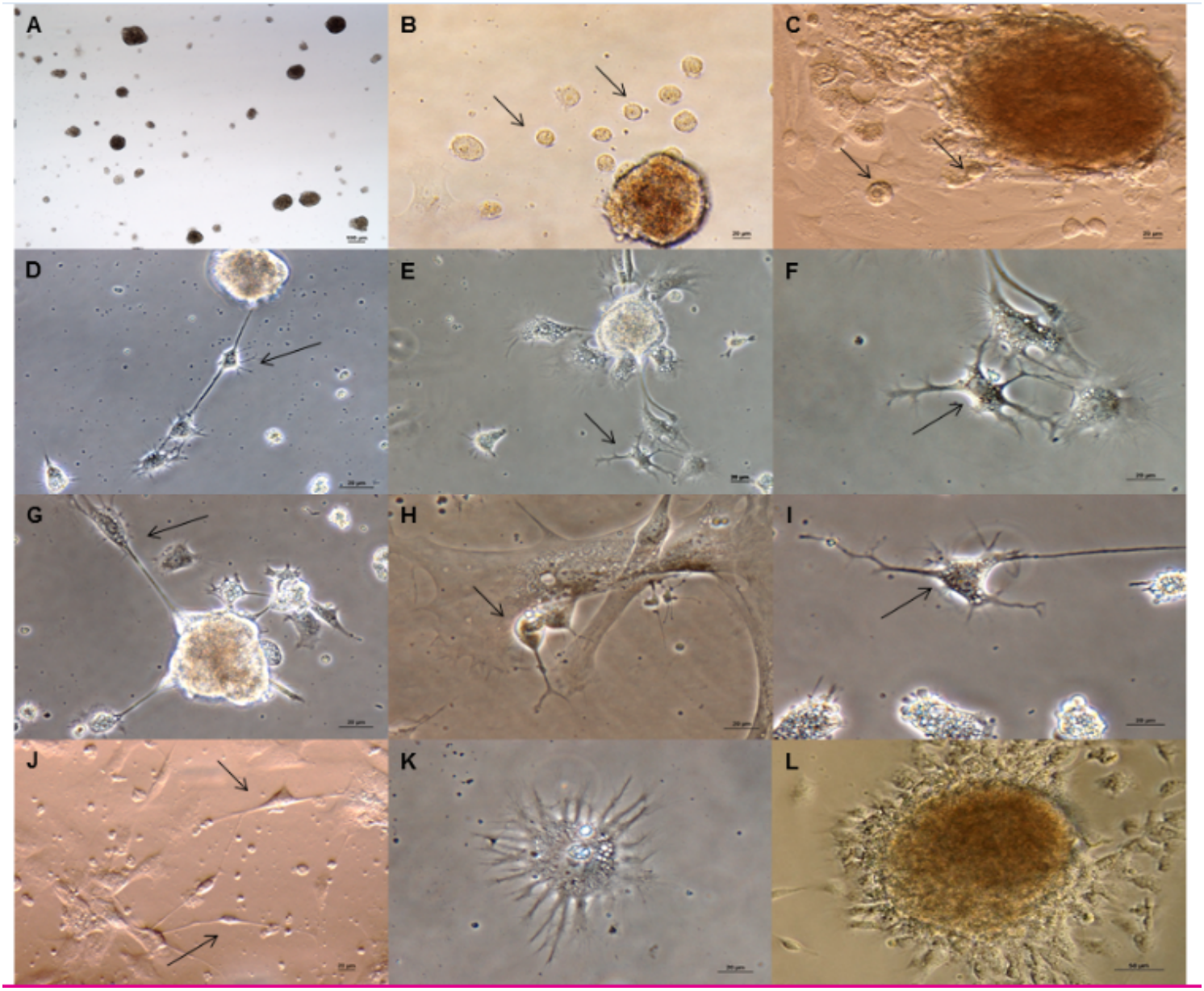

Figure 1

Spontaneous generation of spheroids from sheep ovarian cortical cells. Photomicrographs corresponding to day 7 cell cultures showing (A) spheroids spontenaously derived in vitro from ovarian cortical cells (Plan Achromat 4X/0.10 magnification). During the second week in culture, round cells with a large nucleus to cytoplasm ratio were consistently found arising from these spheroids to migrate towards particular areas of growth surface or aggregating to spheroids (B, 20X/0.40, magnification, phase contrast; C, 20X/0.40 magnification, Hoffman, arrows). These cells eventually exhibited a neural-like morphological differentiation in culture (D, E, G, 20X/0.40 magnification, phase contrast, arrows; F, H, I, K, 40X/0.55 magnification, phase contrast, arrows). An ovarian cortical cells derived spheroid on day 15 in culture, showing polarized cells at its outer sheet cover (L, 20X/0.40, magnification, phase contrast).

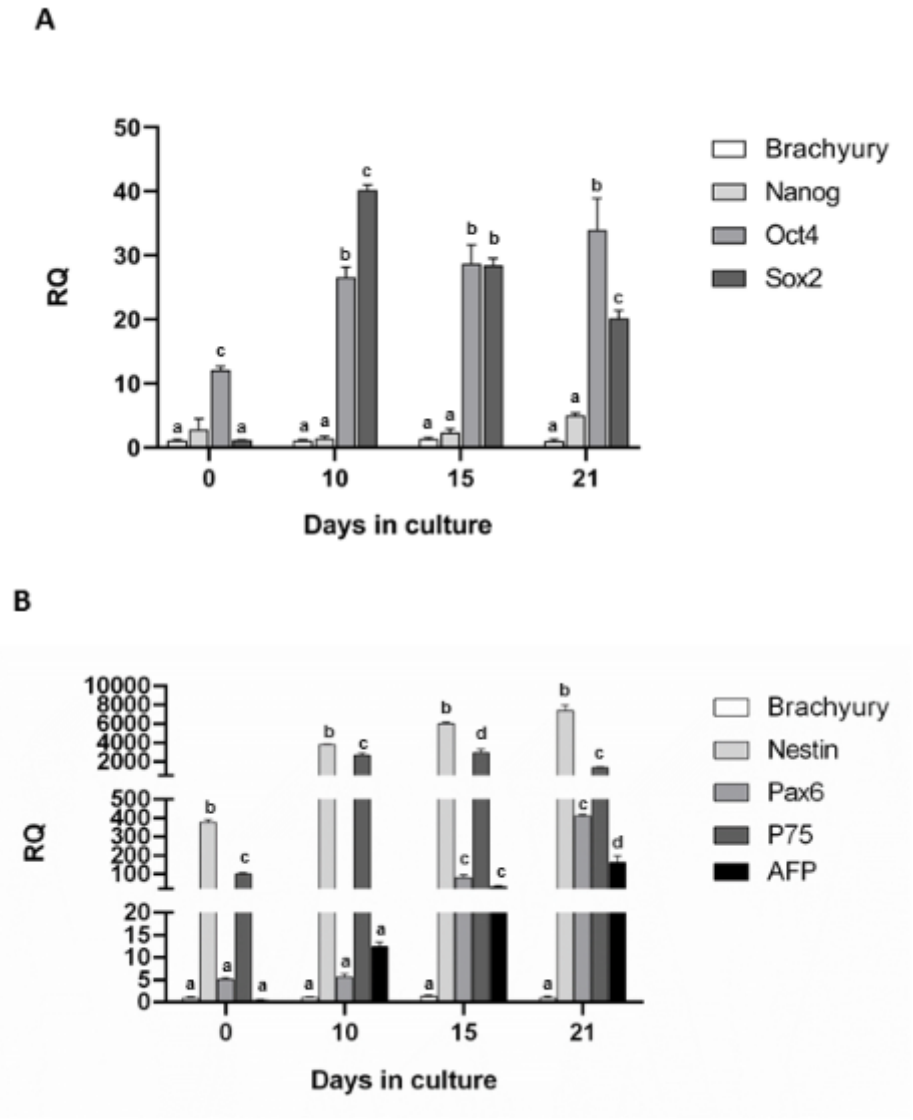

Figure 2

Gene expression analyses of spheroids derived from sheep ovarian cortical cells. Bar graphs depicting the relative quantification (RQ) of transcripts characteristic of pluripotency (A) (Nanog, Oct4 and Sox2), and (B) neuroectoderm (nestin, Sox2, Pax6, p75NTR) and endoderm (AFP, alpha fetoprotein) specification on cell suspension before culture (day 0), and in spheroids on day 10, 15, and 21 of culture. At all time-points, expression of brachyury was considered the reference level of transcription for normalization. In all cases, different numbers indicate significant differences ($P < 0.01$).

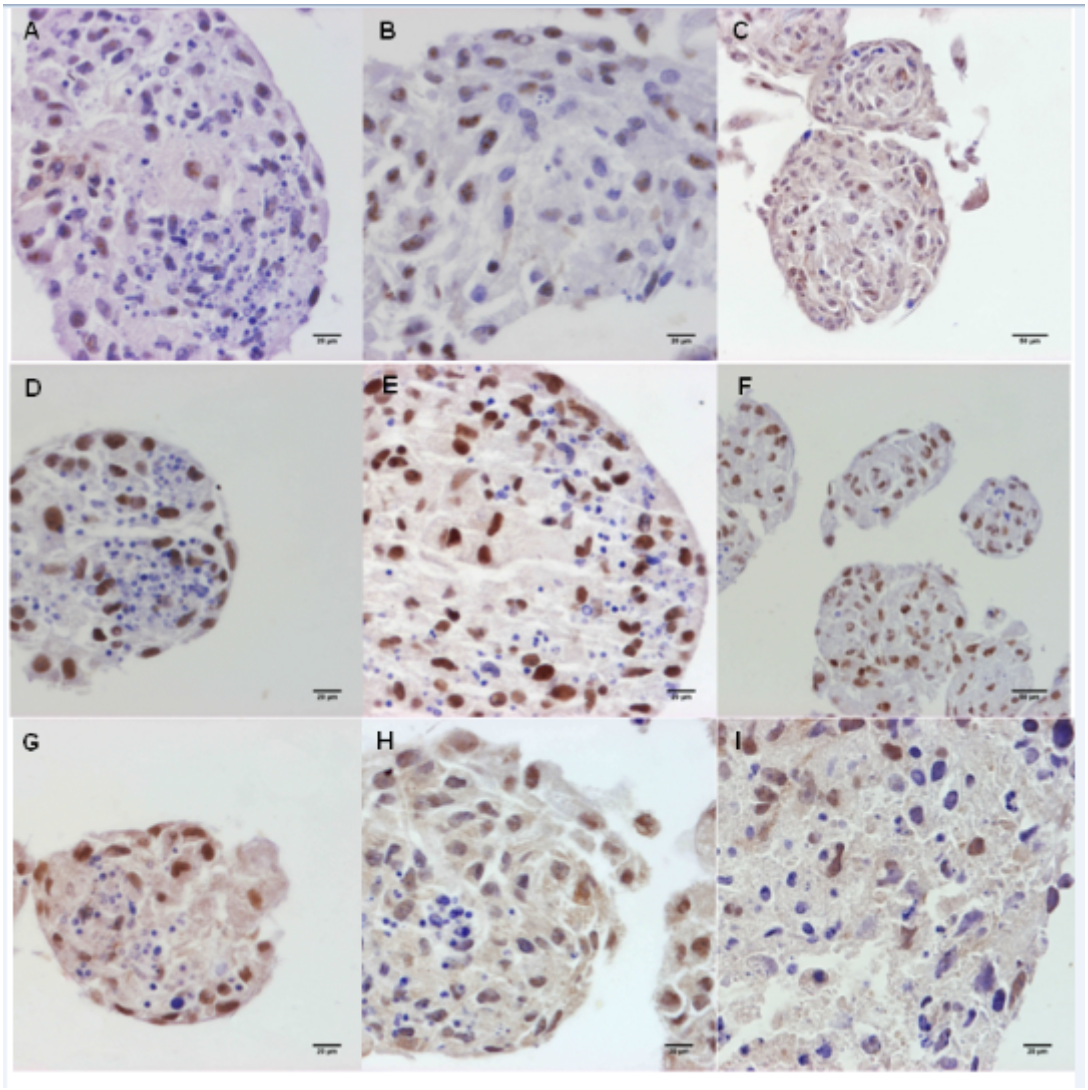

Figure 3

Immunohistochemical localization of NSC/NPC markers in sheep ovarian cortical cells-derived spheroids. Representative photomicrographs of spheroids on day 10 (first column), day 15 (second column) and day 21 (third column) in culture, showing immunoreactivity for nestin (A-C), Pax6 (D-F) and p75NTR (G-I).

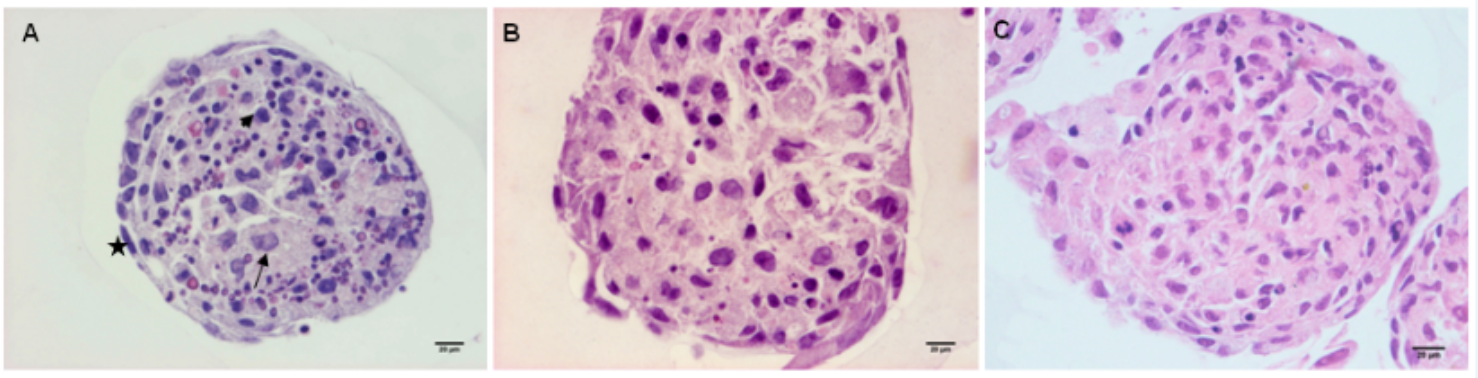

Figure 4

Hematoxilin-Eosin stained sections of sheep ovarian cortical cells-derived spheroids. Light microscopy photomicrographs of spheres with H&E staining. On day 10, spheres are comprised of three subpopulations of cells: large round cells (arrow), intermediate-size cells (arrowhead), and spindle-shaped cells (star). Apoptotic and necrotic cells (small arrows), are frequently observed (A). On days 15 (B), and 21 (C) spheroids became large compact aggregates with the three subpopulations of cells. Signs of cell death were also evident. (H&E staining; 40X magnification).

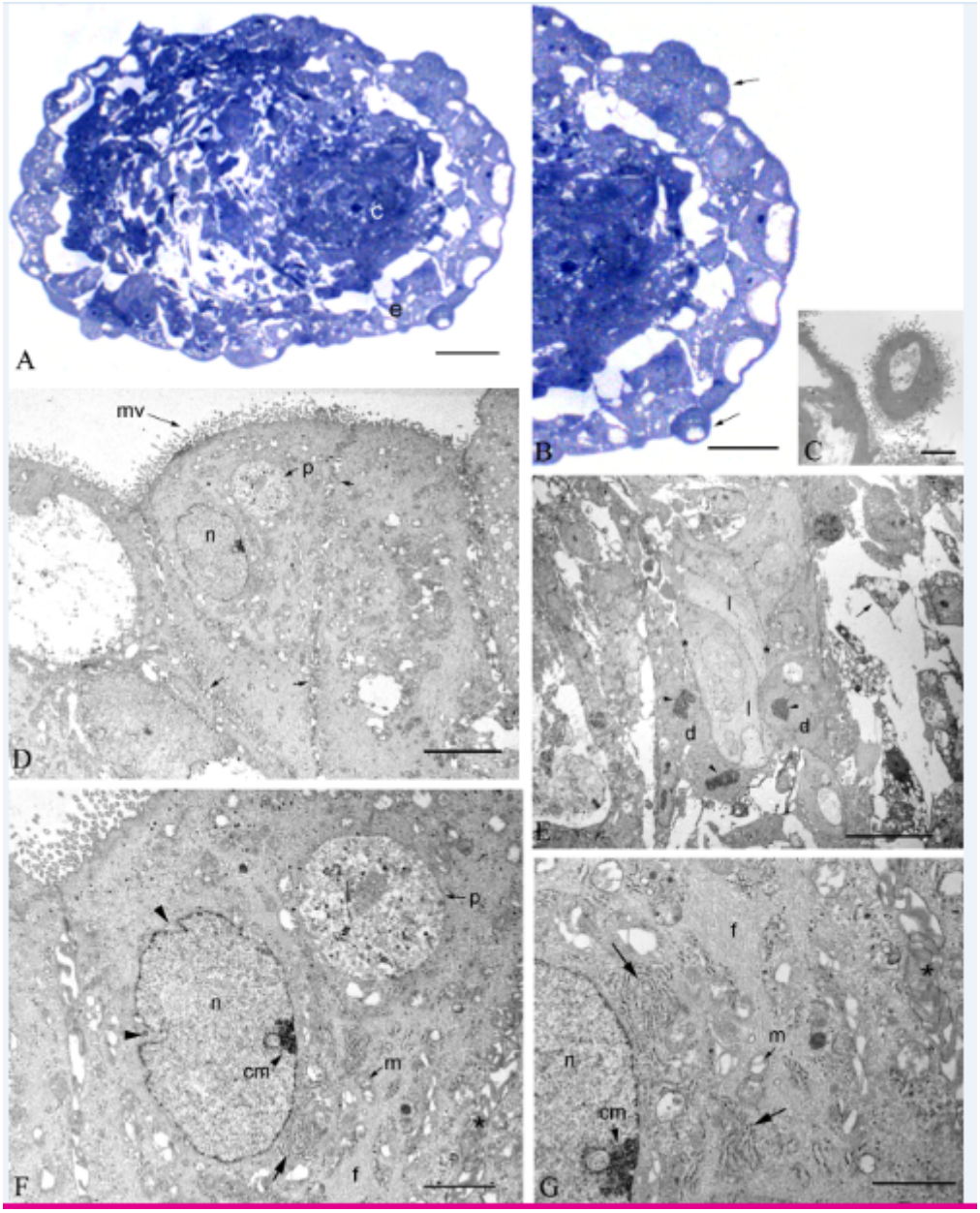

Figure 5

(A-B) Methylene blue-azur-stained semithin sections of spheres. (A) An ovoid sphere on day 15 of culture with two distinct parts, the core (c) and the outer cover or epithelium (e). (B) Higher magnification from Fig. 1A showing the core-epithelium interaction; the epithelium shows both flat and protruding (arrows) apical cells. (C) Electron micrograph showing a protruding cell on day 21 of culture exiting or aggregating with the sphere surface. (D-G) Electron micrographs of spheres on day 15 of culture. (D) Light cells in the

external epithelium of the sphere, bearing apical microvilli (mv); (n) nucleus of light cell; (p) phagosomal vacuole in the cytoplasm of the light cell; (arrows) interdigitated lateral cytoplasmic processes. (E) Core of the sphere with light (l) and dark (d) cells, compacted by apposition of the cytoplasmic membranes (asterisks). Observe the reticulated nuclei of dark cells (arrowheads) and the presence of big intercellular spaces with degenerating (probably apoptotic) figures (arrow). (F,G) Higher magnifications from figure D to show the cytoplasm and nucleus of light cells. The nucleus (n) shows characteristic deep indentations (arrowhead) and condensed chromatin masses (cm) on the nuclear envelop. The cytoplasms of light cells are rich in RER cisternae (arrow), mitochondria (m) (some of them with degenerative signs as swelling and loss of cristae) and intermediate filaments (f); (p) phagosomal vacuole. Bars: 100 µm (A); 50 µm (B); 1 µm (C, G); 5 µm (D); 10 µm (E); 2 µm (F).

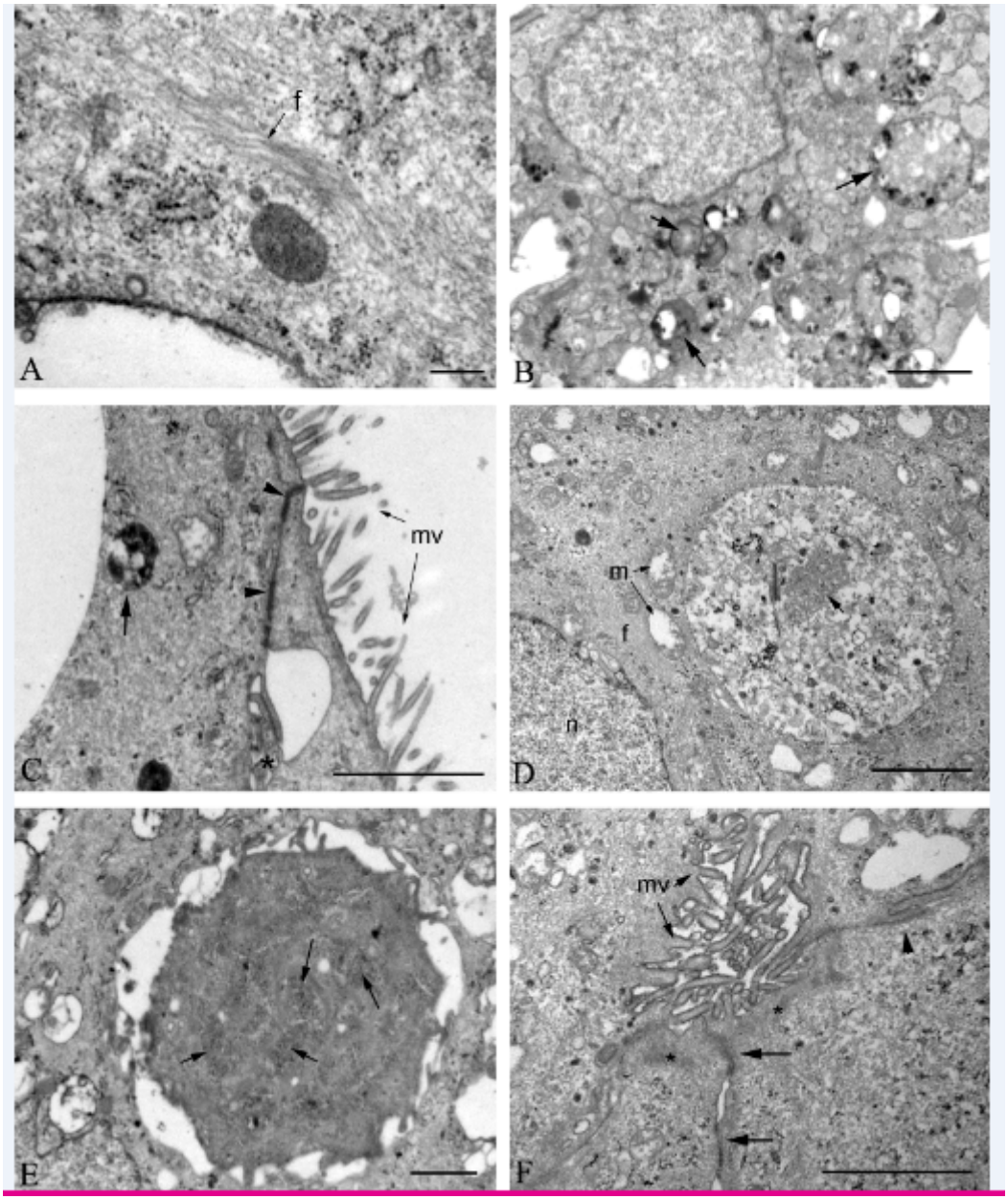

Figure 6

(A-F) Electron micrographs of spheres on day 15 of culture, showing details of light cells. (A) Bundles of intermediate filaments (f). (B) Abundant lysosome and phagosome-like structures (arrows). (C) Lysosome-like structure (arrow) in the cytoplasm of a light cell; (mv) apical microvilli; (arrowheads) adherens junctions between neighbouring light cells; (asterisks) interdigitated lateral cytoplasmic processes. (D) Higher magnification from Fig. 5F to show in detail the phagosomal vacuole, and a recognizable mitochondria inside it (arrow); (n) nucleus of light cell; (m) mitochondria showing signs of swelling; (f) intermediate filaments. (E) Big phagosome in a light cell showing some fragments of, probably, mitochondria (arrows). (F) Apical surfaces of light cells bearing well-developed microvilli (mv); observe a apical tight interdigitation (arrowhead); (arrows) adherens junctions; (asterisks) cytoskeleton elements. Bars: 0.2 µm (A); 1 µm (B, C, D, F); 0.5 µm (E).

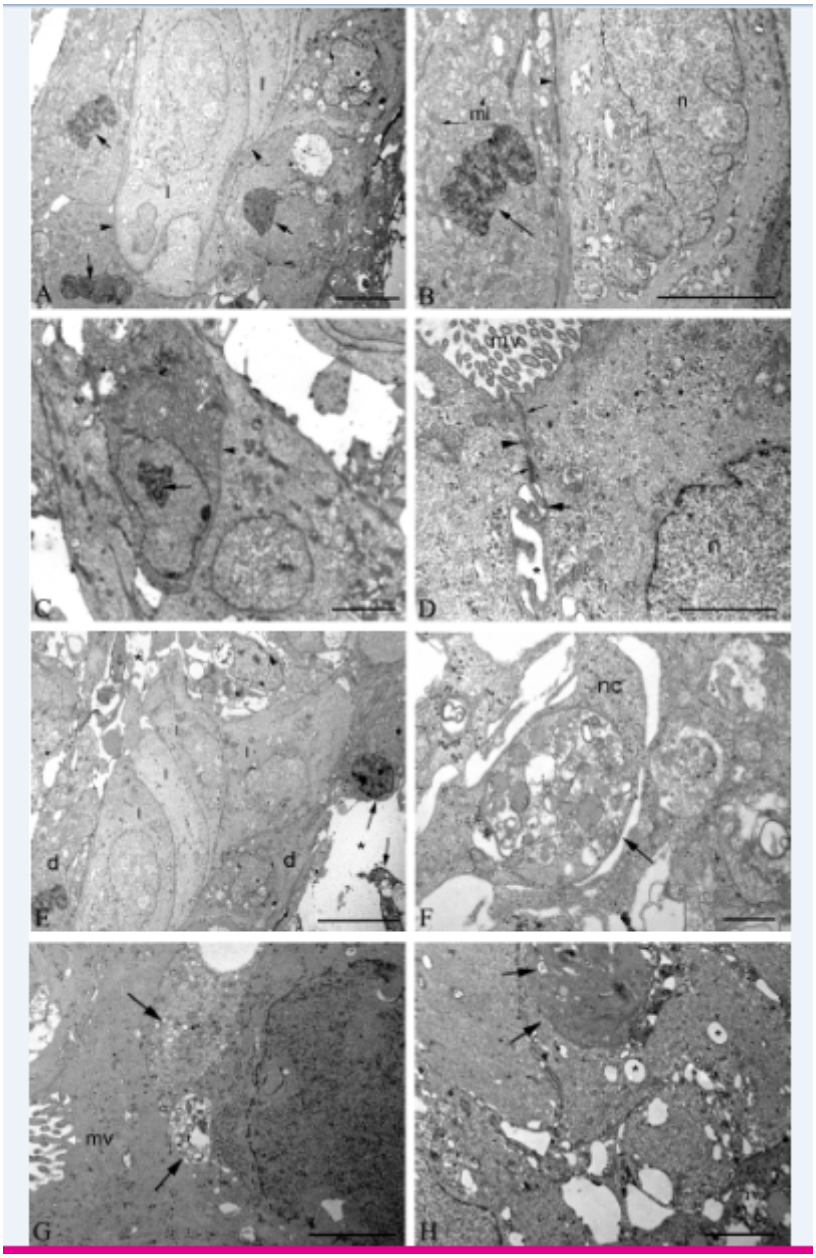

Figure 7

Electron micrographs of spheres on day 15 (A-F) and 21 (G-H) of culture. (A,B,C) Core of the sphere. Dark cells are abundant and show nuclei with reticulated structural configuration (arrows). Cytoplasms of dark cells are rich in large mitochondria (m) (both normal and swollen), and RER cisternae (white arrow).There is apposition of the cytoplasmic membranes between neighbouring cells in the core (arrowheads); (l) light cells; (n) nucleus of the light cell. (D) Cell junctions and contacts between light cells: adherens junctions (small arrows); focal tight interdigitation (arrowhead); (big arrow) cytoplasmic processes loosely interdigitated with those from adjacent cells; (asterisk) wide intercellular clefts; (n) nucleus; (mv) apical microvilli. (E) Degenerating figures, probably apoptotic (arrows) in the core of the sphere; (l) light cells; (d) dark cells; intercellular spaces are abundant (asterisk). (F) Core of the sphere; engulfment of cell debris (arrow) by neighboring cells (nc). (G) Light cells bearing microvilli (mv) are losing intercellular contacts in the periphery of the sphere, and numerous degenerative lysosome-like vesicles occupy the intercellular spaces (arrows). (H) In the core of the sphere is very common to find cytoplasmic vacuoles (asterisks), apoptotic figures and engulfment of cell debris (arrows) by neighboring cells. Bars: 2 μm (A, B, C, G, H); 1 μm (D); 5μm (E); 0.5 μm (F).